598

Reprinted from JOURNAL OF COLLOID AND INTERFACE SCIENCE, Volume 24, No. 4, August 1967

Printed in U.S.A.

JOURNAL OF COLLOID AND INTERFACE SCIENCE 24, 405–415 (1967)

Xenon Adsorption on Graphitized Carbon Blacks over a Wide Coverage Range

H. COCHRANE, P. L. WALKER, JR., W. S. DIETHORN, AND H. C. FRIEDMAN

Pennsylvania State University, Departments of Fuel Science and Nuclear Engineering, University Park, Pennsylvania 16802

Received January 28, 1967

Xenon adsorption isotherms are reported for two graphitized carbon blacks, Sterling MT 3100 and Graphon, at surface coverages ranging from 10^{-10} to 0.9. A radioactive tracer method based on Xe^{133} and a conventional volumetric method were used at the lower and higher coverages, respectively. Results confirm the small degree of surface heterogeneity associated with both materials. Close obeyance of Henry's law over the surface coverage range 10^{-10} to 10^{-6} was observed for Sterling MT 3100. At higher surface coverages, the adsorbed phase on both carbon blacks is interpreted to be a two-dimensionally mobile layer with adsorbate-adsorbate interactions.

I. INTRODUCTION

Graphitized carbon blacks are known to possess predominantly homogeneous surfaces with small amounts of geometric surface heterogeneity (1–4). The heterogeneity is due to surface defects such as vacancies, basal and nonbasal dislocations, (5, 6), and boundaries between intersecting polyhedral faces which compose the surface (7). These defects are strong adsorption sites for gas molecules, and, hence, are the sites where the first gas molecules are adsorbed on carbon surfaces. A study of gas adsorption on graphitized carbon blacks at very low surface coverages promises to show interesting correlations with these defects.

Graham (7) measured N_2 adsorption isotherms at 77.5° and 90.3°K. on two graphitized carbon blacks, Graphon and P-33 (heat treated at 2700°C.), down to surface coverages of 5×10^{-3}. He extrapolated the linear portion of the isotherms to zero pressure and from the positive intercepts estimated that Graphon and P-33 had 1.25% and 0.10% strong sites, respectively. Dietz and coworkers (8) measured adsorption isotherms of N_2 and Ar on mineralogical graphite at 77° to 90°K. down to surface coverages of 3×10^{-3}. Steps in the isotherms indicated a high degree of surface homogeneity.

The measurement of adsorption isotherms at lower surface coverages is desirable, but in conventional adsorption systems utilizing McLeod gages accurate pressure measurement below approximately 10^{-3} torr is difficult. At lower gas pressures, either ultrahigh vacuum systems containing ion gages or a radioactive tracer method, as described in this paper, can be used. Hobson and Armstrong (9) described an ultrahigh vacuum system used to measure N_2 adsorption isotherms on glass at temperatures between 63.3° and 90.2°K. in the relative pressure range 10^{-13} to 10^{-6}, corresponding to surface coverages between 10^{-6} and 0.3.

Radioactive tracers have been used to measure adsorption isotherms at high surface coverages. Clarke (10) developed a radioactive Kr method for the measurement of surface areas from 10^{-3} to 10 $m.^2/g.$, and Chènebault and Schürenkämper (11) used Xe^{133}-labeled Xe for surface areas of a few square centimeters. The radioactive tracer method described in this paper permitted the measurement of Xe adsorption isotherms on two graphitized carbon blacks in the pressure range 10^{-9} to 2 torr, corresponding to

surface coverages of 10^{-11} to 10^{-2}. A conventional volumetric adsorption system was used (12) to extend the isotherms to higher surface coverages.

II. EXPERIMENTAL

The adsorption apparatus (13) used to measure isotherms in the low coverage range consists of four sections: Xe^{133} generation and purification system, radiation detector, Xe doser, and adsorption system. It will be described in some detail, since it has some unique features.

A. Xe^{133} Generation and Purification System. Xe^{133}, a 81-kev. gamma emitter with a half life of 5.27 days, is the radioactive tracer used in this study. This isotope is produced by fissioning U^{235}, in the form of $\sim$1 g. of uranyl nitrate hexahydrate crystals, in a thermal neutron flux of 9×10^{11} n/cm.^{2}/sec. for 2 hours in the Penn State Triga reactor. Eleven radioactive and five stable isotopes of Xe are produced in fission, but after a five-day decay period the only significant radioactive Xe isotope present is Xe^{133}. After an absolute Xe^{133} radioassay, described below, the atom fraction of Xe^{133} in the fission Xe is readily calculated at any later time from the known fission yields (14, 15) and the half life of Xe^{133}. The usual radioactive decay correction was applied to the Xe^{133} radioassays when a single charge of Xe^{133} was used to determine points on the isotherm over a period of several days. Following this five-day decay period, the fission Xe is released from the crystals in a Pyrex purification system by melting the crystals (m.p. 65°C.), after evacuation to 10^{-3} torr, in flowing, high-purity, Matheson He. This gas is dried by passing it through a bed of anhydrous calcium sulfate and Linde 4A molecular sieves before absolute radioassay of Xe^{133} in the radiation detector. One gram of crystals yields about 10^{11} atoms of Xe^{133}.

B. Radiation Detector. The Xe^{133} is measured by counting the 81-kev. photopeak activity with a conventional system consisting of a 2 in. $\times$ 2 in. NaI scintillation crystal, phototube, ratemeter, and single-channel recording spectrometer. Helium carrying Xe^{133}, from either the purification system or the adsorption system, passes at a known rate through a coil of thin-walled aluminum tubing wrapped around the crystal. During the flow, the recorder plots a continuous curve of photopeak activity versus time, and the area under this curve is directly proportional to the number of Xe^{133} atoms in the flowing He.

To calibrate the detector a crystal of uranyl nitrate hexahydrate containing a known amount of Xe^{133} was melted in the purification system and the released Xe^{133} counted as just described. This known Xe^{133} source was prepared by irradiating the crystal in a known thermal neutron flux. The latter was calculated from an absolute radioassay of Co^{60} produced by the $Co^{59}(n, \gamma)Co^{60}$ reaction in a cobalt wire dosimeter irradiated with the crystal. This dosimeter was previously calibrated in this laboratory by comparing it with a known Co^{60} standard. The number of Xe^{133} atoms delivered to the coil in this calibration experiment was calculated from the weight of the crystal, integrated thermal neutron flux, U^{235} fission cross section, Xe^{133} fission yield, and the known kinetics of Xe^{133} daughter growth from precursor fission I^{133}. A few simple experiments established that Xe^{133} release from the molten crystal and its transfer to the radiation detector were quantitative.

The lower limit of Xe^{133} detection in this system is about 1×10^8 atoms. Higher sensitivity can be achieved by using a refrigerated charcoal trap in a well crystal instead of the coil, but this refinement was not necessary in this study.

C. Xenon Doser. For the specified irradiation conditions, Xe pressures higher than 10^{-8} torr cannot be achieved with fission Xe alone in the adsorption system. Natural Xe is added to the fission Xe to provide higher pressures. A doser (16) capable of delivering from 2×10^{10} to 10^{20} atoms of Matheson spectroscopically pure Xe with an accuracy of $\pm 1\%$ was added to the adsorption apparatus for this purpose. This addition allows the measurement of Xe adsorption isotherms at pressures of 10^{-10} to 2 torr.

D. Adsorption System. The Xe^{133} generation and purification system, the flow radiation detector, and the Xe doser are connected to the Pyrex glass adsorption system

as shown in Fig. 1. Here A and B are liquid N_2 refrigerated glass wool traps used to trap out Xe^{133} after it passes through the radiation detector coil. Trapping is quantitative and release of Xe from the trap is complete on removal of the liquid N_2 bath. By manipulating the liquid N_2 baths and reversing the direction of the He flow, the Xe^{133} is passed back and forth through the coil twice, yielding four separate Xe^{133} determinations which, in general, differ no more than $\pm 4\%$; the inherent uncertainty is the determination of recorder chart area. The average of the four determinations defines the Xe^{133} radioassay. Tubes C and D are refrigerated with dry ice/acetone and contain rolls of copper foil which remove traces of organic vapor (17) possibly introduced into the He by the stopcocks, etc. Mercury valves containing triply distilled mercury are used elsewhere to eliminate sources of organic vapors in the adsorption system. A glass wool trap E serves the same purpose as A and B, F is a 100-ml. gas buret, and G is a Hg manometer used only to make the initial volume calibration of the apparatus with He. The absorbent is located in the adsorption bulb H. Mercury contamination of the absorbent is minimized by placing a dry ice/acetone bath around the U-tube I.

E. Experimental Procedure. Samples of Sterling MT 3100 (6 g.) or Graphon (1 g.), both highly graphitized carbon blacks of 7.7 and 89.7 $m.^2/g.$ area (N_2 BET measurement), are placed in the adsorption bulb H and held at 300°C. for 48 hours while the adsorption system is evacuated to 10^{-6} torr. Xe^{133}, previously radioassayed, is passed through trap D and collected in trap E with valves M_2, M_6, and M_1 open and valves M_4 and M_8 shut. Valves M_2 and M_1 are then shut and the He carrier gas is pumped out of the system via valve M_8. Valve M_8 is then closed and valve M_4 opened. Liquid N_2 baths are placed around trap I and bulb H and removed from trap E, allowing the fission Xe to diffuse into the adsorption bulb. Diffusion is complete in 2.5 hours.

A known amount of natural Xe is then added to the adsorption system from the doser and collected in the refrigerated adsorption bulb. The liquid N_2 baths are then removed from I and bulb H, and the fission and natural Xe allowed to mix for 4 hours. Trap I is then refrigerated with dry ice/acetone, and a temperature bath corresponding to the desired isotherm temperature is placed around the adsorption bulb.

After adsorption equilibrium is attained (this was found experimentally to take 3.5 hours), valve M_4 is shut, and the Xe contained in the adsorption apparatus to the

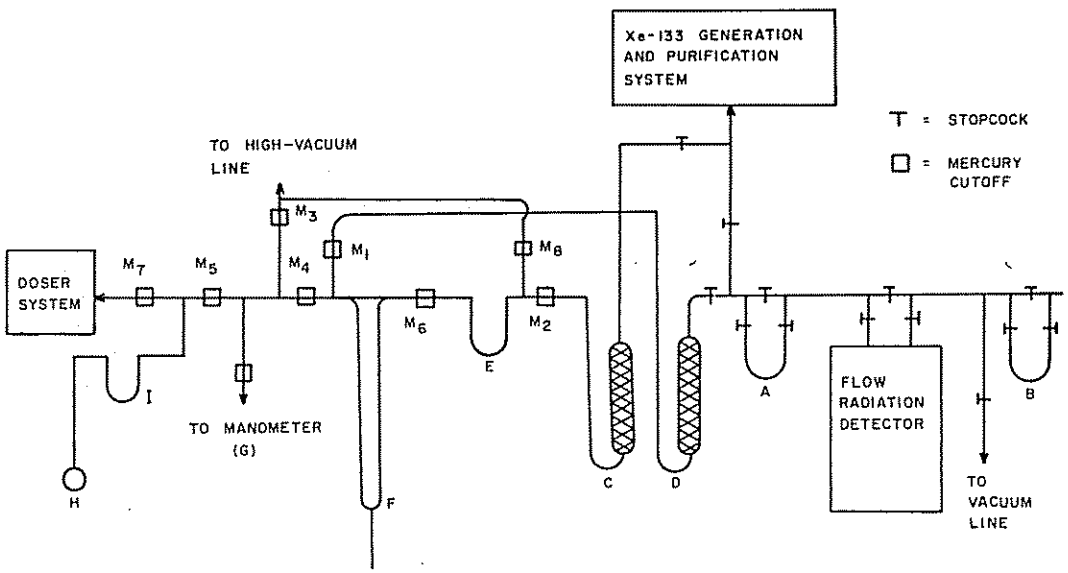

FIG. 1. Adsorption system

right of this valve is collected in trap E prior to passing it through the coil in flowing He for radioassay of the Xe^{133}. After radioassay, this sample is discarded. The total amount of Xe in equilibrium with the adsorbent is calculated from the known fraction of the total adsorption system dead space from which the radioassayed Xe^{133} was taken. This quantity and the initial amount of Xe^{133} and natural Xe charged into the system give the Xe pressure in equilibrium with the absorbent, and the amount on the absorbent. The section of the adsorption system from which this last sample of Xe was taken is now evacuated to 10^{-6} torr, valve M_4 is opened, and the system allowed to re-equilibrate at a lower adsorption pressure. This process is repeated until the Xe^{133} concentration in the Xe removed from the adsorption system is too low to measure. The entire adsorption system is then evacuated to 10^{-6} torr, and adsorption measurements are made in another pressure range by adding a new sample of Xe^{133} and a new sample of natural Xe, but at a different pressure, to the adsorption system. In this manner complete adsorption isotherms over the Xe pressure range 10^{-9} to 2 torr are obtained.

Xenon adsorption isotherms were measured at −78°, −89.5°, −100°, and −111°C., corresponding to temperature baths of dry ice/acetone, solid/liquid *n*-propyl alcohol, solid/liquid methyl alcohol, and solid/liquid *n*-butyl bromide. The dry ice/acetone bath was prepared by adding crushed ice to a Dewar of acetone; the latter three baths were obtained by adding liquid N_2 to the respective liquids. By careful attention to technique, the bath temperatures, as measured by a copper-constantan thermocouple attached to the sample bulb, could be held to the fixed temperatures within ±0.5°C. throughout the adsorption time.

F. Additional Comments on Method. Several factors which could have affected the isotherms are discussed below.

1. *Thermal transpiration correction.* Adsorption pressures were corrected for thermomolecular flow between the adsorption bulb and the remainder of the apparatus using Liang's equation (18) or the Knudsen correction, depending on the absolute Xe pressure.

2. *Reversibility.* The measured isotherms are desorption rather than adsorption isotherms, that is, the adsorbent is equilibrated at the highest pressure first and then with successively lower pressures until the Xe^{133} is too low to measure. The possibility of hysteresis in the isotherms in the low coverage range studied here is unlikely. Hysteresis due to capillary condensation, even in solids containing very fine pores, occurs at coverages above one monolayer (19) or at relative pressures above 0.1. Hysteresis at lower coverages is expected when chemisorption occurs, but chemisorption is not expected when Xe is used as the adsorbate. Sterling MT 3100 has a very low porosity (20). Indeed, even NH_3 isotherms on Sterling MT 3100 showed hysteresis effects only above a relative pressure of 0.4. Hence, the isotherms are referred to throughout this paper as adsorption isotherms.

3. *Mercury contamination.* If mercury contaminated the adsorbent and, hence, affected the isotherms, it could not be detected. Points in the lowest coverage region of the isotherms could be reproduced within ±3% with different Xe charges separated in time by ten days. The dry ice/acetone bath on trap I reduced the mercury pressure in the vicinity of the sample to 6×10^{-9} torr.

4. *Air leakage into adsorption system.* The adsorption system was never evacuated to a pressure lower than 10^{-6} torr, so there was always some background pressure of air in the system which increased slowly during adsorption runs with a single charge of Xe. The background pressure buildup with time in the volume enclosed by mercury valves M_7, M_3, and M_6 was compared with that in the volume not containing the adsorption bulb, that is, enclosed by valves M_5, M_3, M_1, and M_6. The rates of pressure buildup in the two cases were almost identical, showing that outgassing of the carbon blacks is not the dominant source of foreign gases in the adsorption system. Determination of three or four points on an isotherm with a single charge of Xe took about five days. Air pressure in the ad-

sorption system increased from 10^{-6} to 10^{-4} torr during this time. All isotherm temperatures are above the critical temperatures of O_2 and N_2. The relative pressures of O_2 and N_2 exceed the relative Xe pressure only in the very low coverage region of the isotherms. On the basis of these facts, the Xe is expected to compete very favorably with O_2 and N_2 for the available adsorption sites. The reproducibility of the isotherms discussed earlier indicates that if air does influence Xe adsorption the effect is not cumulative.

5. *Adsorption of krypton.* Four stable and twelve short-lived isotopes of Kr are produced in U^{235} fission, but only the former are present in any significant amount in the Xe^{133} charged into the adsorption system. The ratio of total stable Xe to total stable Kr is 5. When natural Xe is added to the fission Xe, this ratio is much higher. Therefore, only at Xe pressures below 10^{-8} torr, where fission Xe alone is used, would any possible effect due to Kr be of concern. Even at the lowest pressures studied Xe will be preferentially absorbed because Kr has a critical temperature of −63°C. compared to 17°C. for Xe^{22}. Below 10^{-8} torr the relative pressure of Kr is 100 times smaller than the relative pressure of Xe.

III. RESULTS AND DISCUSSION

A. Experimental Isotherms. The low pressure Xe isotherm data on Sterling MT 3100 and Graphon are shown in Figs. 2 and 3. The data are plotted on a logarithmic scale because of the wide pressure range studied. Pressures are plotted in absolute rather than relative units to emphasize the very small lower limit of Xe pressures at which these measurements were made. The logarithmic plots have a slope very nearly equal to unity indicating the close obeyance of the data to Henry's law.

Figures 4 and 5 show the adsorption isotherms of Xe on Sterling MT 3100 and Graphon at higher pressures. Points on two isotherms, Sterling MT 3100 at −78°C. and Graphon at −111°C, were determined by both adsorption and desorption, and show complete reversibility. At these temperatures, the vapor pressures of Xe are 3200

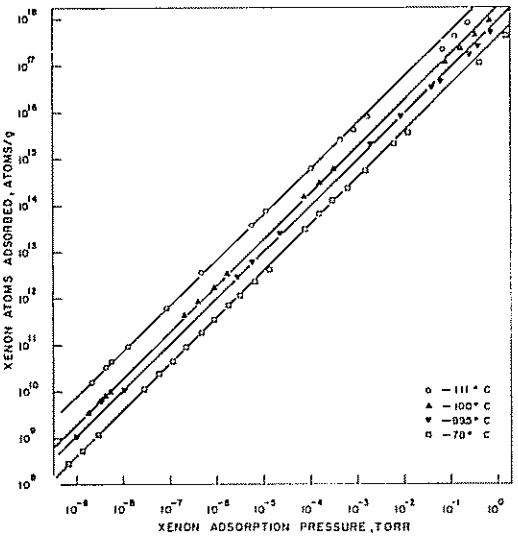

FIG. 2. Xenon adsorption isotherms on Sterling MT 3100 at low surface coverages.

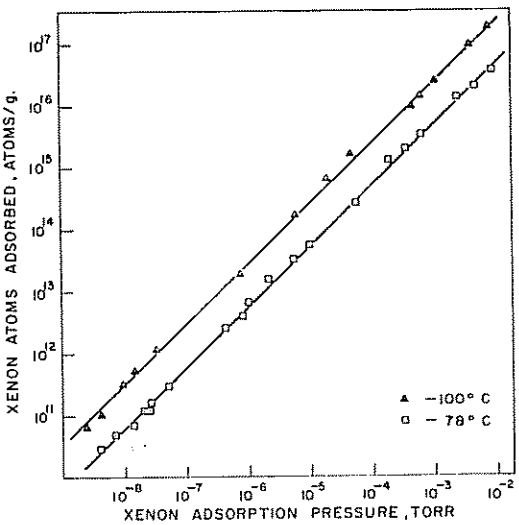

FIG. 3. Xenon adsorption isotherms on Graphon at low surface coverages.

and 637 torr, respectively. The corresponding maximum relative pressures for these two isotherms are 0.08 and 0.36.

B. Heats of Adsorption. Isosteric heats of adsorption, $q_{st} \pm 0.05$ kcal./mole, were calculated from the isotherms of selected values of surface coverage θ by least squares using the Clapeyron-Clausius equation. The plots of ln p against $1/T$ were linear, showing the internal consistency of the iso-

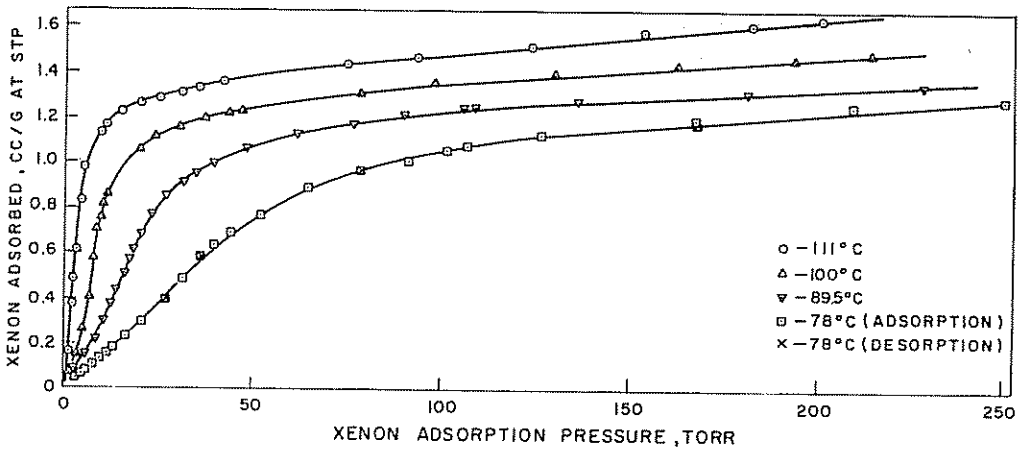

FIG. 4. Xenon adsorption isotherms on Sterling MT 3100 at higher surface coverages

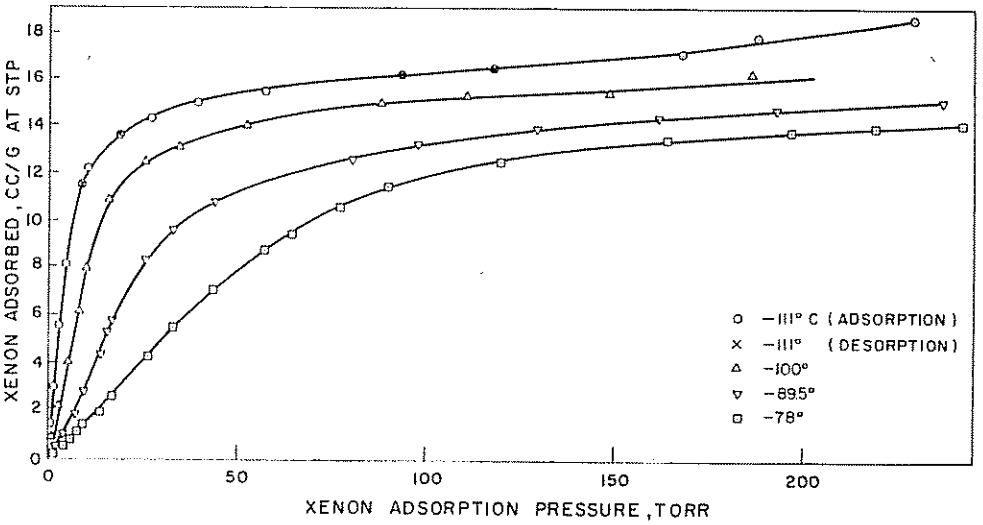

FIG. 5. Xenon adsorption isotherms on Graphon at higher surface coverages

therms and the constancy in the isosteric heats of adsorption over the temperature range studied. A molecular area of 24.0 A^2 was assumed for Xe^{23} in the calculation of θ.

Figure 6 shows the variation in q_{st} with surface coverage on Sterling MT 3100 and Graphon in the low coverage range. At the lowest surface coverages studied, about 3.1×10^{-10} of a monolayer, the maximum heat of adsorption is 4.8 kcal./mole for Sterling MT 3100 and 5.1 kcal./mole for Graphon. For both samples the plots have slopes of about −0.1 kcal./mole per cycle of coverage, indicating a very small dependence of q_{st} on coverage. It indicates that the extent of heterogeneity, even in this low coverage range, is very low.

Figures 7 and 8 show the variation in q_{st} with surface coverage over the range $\theta = 3.1 \times 10^{-10}$ to 0.9. These plots are very similar and indicate that the two graphitized carbon blacks have basically homogeneous surfaces with slight degrees of geometric heterogeneity. The more homogeneous the surface is, the lower the value of θ_m, the value of θ at the minimum q_{st} (7). The minimum q_{st} occurs at θ_m = about 0.025 for Sterling MT 3100 and θ_m = about

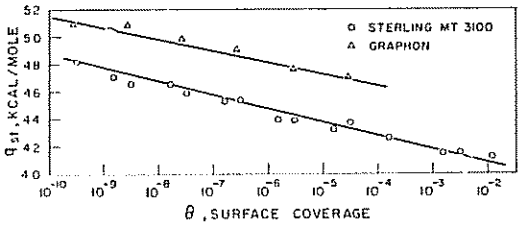

FIG. 6. Variation of isosteric heats of adsorption of xenon on graphitized carbon blacks at low surface coverages.

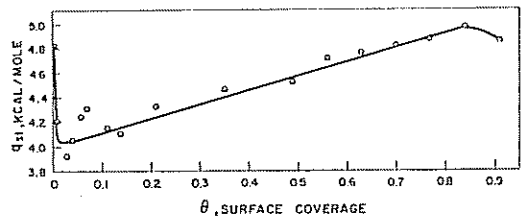

FIG. 7. Variation of isosteric heat of adsorption of xenon on Sterling MT 3100 up to high coverages.

0.05 for Graphon. For $\theta < \theta_m$, q_{st} decreases with increasing θ because of surface heterogeneity. For $\theta > \theta_m$, q_{st} increases with increasing θ because of adsorbate-adsorbate interaction.

The homotatic nature of the two carbon black surfaces, suggested by the isotherms, is understandable on the basis of electron microscope studies. The generally accepted structure for the graphitized blacks is that suggested by Kuroda and Akamatu (24). Each particle consists of a number of pyramidal-shaped graphite crystals with their apices directed towards the center of the particle. The surface of the particle exposed to an adsorbing gas consists almost entirely of the graphite basal plane with little prismatic surface exposed.

Few adsorption studies have been made on carbon using Xe as an adsorbate. Cannon and co-workers (25) obtained isosteric heats of adsorption for Xe on AGOT grade graphite of from 3500 to 3700 cal./mole over the surface coverage range 5.0×10^{-3} to 2.5×10^{-2}. Halsey and co-workers (26) estimated, by extrapolation, a value of 4059 cal/mole for Xe adsorbed on graphitized P-33 at zero coverage. They extrapolated from a region in which the P-33

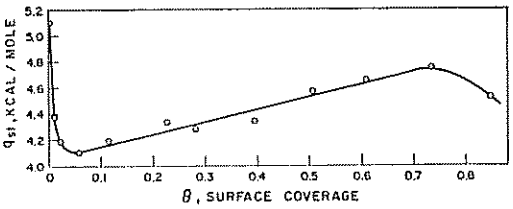

FIG. 8. Variation of isosteric heat of adsorption of xenon on Graphon up to high coverages.

surface was homogeneous and deliberately did not take into account the heterogeneous surface region at low surface coverage. All values of the isosteric heat of Xe on graphitized carbons lie within the generally accepted range for physical adsorption of one to two times the heat of vaporization of Xe liquid, 3270 cal./mole (27).

C. Entropy of Adsorption. Values of the entropy of adsorption ΔS_θ were calculated for different surface coverages using the equations

$$\Delta F_\theta = -RT \ln \frac{p_0}{p_\theta},$$

$$\Delta F_\theta = \Delta H_\theta - T\Delta S_\theta.$$

Here ΔF_θ is the change in free energy of the adsorbate at pressure p_θ in going from the gaseous to the adsorbed state at temperature T, p^0 is the standard pressure (1 atm.) in the gas state, and ΔH_θ is the isosteric enthalpy of adsorption at surface coverage θ.

With these values of ΔS_θ, the entropy models and equations of de Boer and Kruyer (28) were used in an attempt to establish the nature of the adsorbate film at surface coverages below a monolayer. De Boer and Kruyer considered two entropically ideal states. In the model of an ideal mobile monolayer, they assume that the original translational entropy of an ideal gas (gS_{tr}) is transformed to the translational entropy of an ideal two-dimensional gas (aS_{tr}) on the surface of a solid with the loss of one mode of translational entropy, but with the internal vibrations and rotations of the molecules in the gas and adsorbed states remaining unchanged. For the model of an immobile monolayer, they assumed that all three modes of translational entropy of the gas molecule are lost

on being adsorbed and again the internal vibrations and rotations of the molecules in the two states remain unchanged. Using our experimental values of ΔS_θ we calculated values of $\Delta S_{m(\exp)}$ and $\Delta S_{im(\exp)}$, the difference in differential entropy between the three-dimensionally mobile gas in its standard state and the standard states of the mobile and immobile adsorbed monolayers, respectively. The two equations derived by de Boer and Kruyer for the two adsorbed states are

$$\Delta S_{m(\exp)} = \Delta S_\theta + R\, ln\, \frac{A^0}{A};$$

$$\Delta S_{im(\exp)} = \Delta S_\theta + R\, ln\, \frac{\theta}{1-\theta}$$

The standard state of the mobile film is so defined that the average distance of separation A^0 at 0°C. is the same as in a three-dimensional gas at standard temperature and pressure, i.e., 33.9×10^{-8} cm. At any other temperature T the standard molecular area A^0 is $4.08 \times 10^{-16}T$ cm. The standard state condition for the immobile film is taken as $\theta = \frac{1}{2}$.

Theoretical values of ΔS_m and ΔS_{im} were calculated using the entropy relationships

$$-\Delta S_{im(\text{th})} = gS_{tr};$$

$$-\Delta S_{m(\text{th})} = gS_{tr} - aS_{tr}.$$

The standard molar entropy of an ideal gas is given by the Sackur Tetrode equation

$$gS_{tr} = R \ln (M^{3/2}T^{5/2}) - 2.30,$$

where M is the mass of the adsorbate molecule and T is the absolute temperature. De Boer and Kruyer derived a value for aS_{tr} using the model of an ideal adsorbed gas and a surface pressure of 0.338 dyne/cm. as the standard state for the adsorbed monolayer.

$$aS_{tr} = 0.67\ \tfrac{2}{3}gS_{tr} + 1.52 \log_{10}T - 3.04.$$

The entropy calculations for Xe adsorbed on Sterling MT 3100 are shown in Table I. They suggest that the adsorbate film is best represented by the model of a two-dimensional gaseous film of Xe. The same conclusion is reached when our Graphon results are examined in this way.

TABLE I

ENTROPIES FOR XENON ADSORBED ON STERLING MT 3100 AT −78°C.

θ	ΔH_θ (kcal./mole)	ΔS_θ (cal./deg./mole)	$-\Delta S_{im(\exp)}$ (cal./deg./mole)	$-\Delta S_{m(\exp)}$ (cal./deg./mole)
3.1×10^{-10}	4.81	23.33	20.93	13.16
3.1×10^{-9}	4.65	19.54	19.33	12.18
3.1×10^{-8}	4.58	15.33	18.97	12.02
3.1×10^{-7}	4.53	11.02	18.71	11.76
3.1×10^{-6}	4.37	7.22	17.94	11.01
3.1×10^{-5}	4.38	2.42	18.17	11.22
3.1×10^{-4}	4.15	−1.18	17.20	10.25
1.6×10^{-3}	4.14	−4.49	17.32	7.62
2.2×10^{-2}	3.92	−9.30	16.34	9.68
5.6×10^{-2}	4.24	−12.36	17.96	11.36
1.1×10^{-1}	4.15	−13.03	17.19	10.65
2.1×10^{-1}	4.33	−15.36	17.93	11.70
4.9×10^{-1}	4.52	−17.08	17.17	11.78
7.0×10^{-1}	4.82	−20.48	19.45	14.47
9.1×10^{-1}	4.86	−21.01	16.41	14.47

gS_{tr} = 38.39 cal./deg./mole. $gS_{tr} - aS_{tr}$ = 12.36 cal./deg./mole.

Ross and Pultz (29), using the de Boer and Kruyer equations, found good agreement of their data on adsorbed monolayers of Ar and N_2 on boron nitride and graphitized carbon black with the two-dimensional gaseous film model. Values of $\Delta S_{m(\exp)}$ lower than the theoretical value of $gS_{tr} - aS_{tr}$ at coverages between 3.1×10^{-9} and 4.9×10^{-1} may be attributed to retention of part of the lost mode of translation perpendicular to the surface as a vibrational mode perpendicular to the surface. Kemball termed this adsorbed condition "the super mobile condition" (30). This condition was previously found by de Boer and Kruyer for Ar adsorbed on charcoal at temperatures above 200°K. and for Hg on charcoal at 66°K. Values of $\Delta S_{m(\exp)}$ greater than the theoretical value of $gS_{tr} - aS_{tr}$ at higher coverages are attributed to a restriction in translational freedom of the Xe atoms over the adsorbent surface. However, neither of these arguments explains the somewhat high values of $\Delta S_{m(\exp)}$ observed on both carbon blacks at the lowest coverages studied.

D. Theoretical Considerations of Adsorption Isotherms. The most significant feature of the isotherms reported in this paper is

their close obeyance to Henry's law at low surface coverages. Young and Crowell (31) have listed several papers in which linear isotherms have been found at low surface coverages but suggest that the ranges of coverage studied were not sufficiently large to prove linearity. This criticism cannot be leveled at the data reported here, since Henry's law fits the adsorption data closely over a wide surface coverage range, that is, 10^{-10} to 10^{-6}. Over this coverage range, the Henry's law constants for Sterling MT 3100 and Graphon increase by 4% and 20%, respectively. We think this close obeyance to Henry's law is consistent with the fact that only slight surface heterogeneity exists in this coverage range, as concluded from our q_{st} data. However, it is perhaps pertinent that Hill (32) has shown theoretically it is possible for Henry's law to be obeyed on heterogeneous surfaces at low coverages.

Steele (33) suggests defining an activity coefficient for one-component adsorbed layers in the Henry's law region as

$$f(\theta) = p/N_a K_H ,$$

where N_a is the amount adsorbed per unit area and K_H is the Henry's law constant for $N_a \to 0$. According to Steele, deviations in $f(\theta)$ from its limiting value of unity are due only to lateral attractions and repulsions between adsorbed atoms. Further,

$$\bar{F}_a - \bar{F}_{a(\mathrm{id})} = RT \ln f(\theta);$$

$$\bar{\Pi}_a - \bar{\Pi}_{a(\mathrm{id})} = \Delta H_{st}(\theta) - \Delta H_{st}(0).$$

Here $\bar{F}_a - \bar{F}_{a(\mathrm{id})}$ and $\bar{\Pi}_{a(\mathrm{id})}$ represent differences between properties of the real adsorbed layer and the ideal adsorbed layer. Table II contains values for $f(\theta)$, $\bar{\Pi}_a - \bar{\Pi}_{a(\mathrm{id})}$, and $S_a - \bar{S}_{a(\mathrm{id})}$ for Xe adsorption at −78°C. on the two graphitized blacks. The activity coefficient $f(\theta)$ is set equal to one at the lowest coverage studied to calculate K_H. Over a similar range of N_a, it is seen that the activity coefficient rises more rapidly on Graphon than on Sterling MT 3100.

An attempt was made to fit the adsorption data at coverages where adsorbate interaction is significant, that is, at coverages greater than θ_m in Figs. 7 and 8, by an appropriate theoretical equation. Since the entropy data showed that the adsorbed phase was a mobile two-dimensional gaseous film, the adsorption isotherm derived by Hill (32, 34) for mobile monolayers with interaction was used.

$$p = \kappa \frac{\theta}{1-\theta} \exp\left[\frac{\theta}{1-\theta} - \frac{2\alpha\theta}{\beta RT}\right].$$

Here α and β are values of the energy of adsorbate-adsorbate interaction and the area occupied by an adsorbate molecule in a complete monolayer, respectively; κ involves a

TABLE II

DEVIATION FROM IDEALITY FOR XENON ON GRAPHITIZED CARBON BLACKS IN LOW COVERAGE RANGE AT −78°C.

θ	N_a (atoms/m.²)	p (torr)	$f(\theta)$	$\bar{\Pi}_a - \bar{\Pi}_{a(\mathrm{id})}$ (kcal./mole)	$\bar{S}_a - \bar{S}_{a(\mathrm{id})}$ (cal./deg./mole)
		Sterling MT 3100			
3.1×10^{-10}	1.3×10^{9}	2.45×10^{-8}	1.00	0	0
3.1×10^{-9}	1.3×10^{10}	2.50×10^{-7}	1.02	+0.16	+0.78
3.1×10^{-8}	1.3×10^{11}	2.50×10^{-6}	1.02	+0.23	+1.14
3.1×10^{-7}	1.3×10^{12}	2.50×10^{-5}	1.02	+0.28	+1.39
3.1×10^{-6}	1.3×10^{13}	2.55×10^{-4}	1.04	+0.44	+2.21
3.1×10^{-5}	1.3×10^{14}	2.75×10^{-3}	1.12	+0.43	+2.16
		Graphon			
2.7×10^{-10}	1.1×10^{9}	1.65×10^{-8}	1.00	0	0
2.7×10^{-9}	1.1×10^{10}	1.77×10^{-7}	1.07	+0.02	−0.03
2.7×10^{-8}	1.1×10^{11}	1.87×10^{-6}	1.13	+0.12	+0.37
2.7×10^{-7}	1.1×10^{12}	2.00×10^{-5}	1.21	+0.20	+0.64
2.7×10^{-6}	1.1×10^{13}	2.07×10^{-4}	1.25	+0.35	+1.35

number of terms, but is independent of θ. This equation can be rearranged in the form

$$\ln \frac{\theta}{1-\theta} - \ln p + \frac{\theta}{1-\theta} = -\ln \kappa + \frac{2\alpha\theta}{\beta RT}.$$

The left-hand side of this equation was plotted against θ for each adsorption isotherm. Linear plots were obtained on both graphitized blacks at surface coverages from $\theta = 0.05$ to 0.5 at all adsorption temperatures studied. From the slopes of the plots, values of $2\alpha/\beta$ were determined. From the equation $T_{2c(\mathrm{app})} = 8\alpha/27\beta R$ (31) apparent two-dimensional gas critical temperatures were calculated. The intercept of the plots gave values of κ. Results are given in Table III for the two graphitized blacks.

The two-dimensional critical temperature for a gas has been shown theoretically to be one-half the gas phase critical temperature T_{3c} (34, 35). Kobe and Lynn (22) determined a value of T_{3c} of 289.7°K. for Xe, so $T_{2c(\mathrm{th})}$ for Xe is 144.9°K. They report that the values of $T_{2c(\mathrm{app})}$ calculated for Xe on graphitized carbon blacks are somewhat lower than the theoretical value. This is also usually the case for other gases and solids (31). Ross and Clark (36) found a value of $T_{2c(\mathrm{app})} = 104$°K. for Xe on sodium chloride crystals. Our $T_{2c(\mathrm{app})}$ values for Sterling MT 3100 are significantly higher than those for Graphon; further the former are less sensitive to adsorption temperature than the latter. The average value of $T_{2c(\mathrm{app})}$ on Sterling MT 3100 is 120.6°K. A higher value of $T_{2c(\mathrm{app})}$ on MT 3100 than on Graphon is consistent with the smaller amount of heterogeneity in the former.

TABLE III

PARAMETERS DESCRIBING XENON ADSORPTION IN THE INTERMEDIATE COVERAGE RANGE ON GRAPHITIZED CARBON BLACKS

Adsorption temperature (°C.)	$2\alpha/\beta$ (joules/mole $\times 10^{-3}$)	$T_{2c(\mathrm{app})}$ (°K.)	κ (atm.)
	Sterling MT 3100		
−78	6.523	116.2	0.159
−89.5	7.116	126.8	0.103
−100	6.912	123.2	0.048
−111	6.526	116.3	0.020
	Graphon		
−78	6.134	109.3	0.156
−89.5	6.109	108.9	0.082
−100	5.759	102.6	0.037
−111	4.450	79.3	0.014

TABLE IV

AVERAGE AREAS OCCUPIED BY XENON ATOMS IN COMPLETE MONOLAYER ON GRAPHITIZED CARBON BLACKS

Adsorption temperature (°C.)	Areas (A^2)	
	Sterling MT 3100	Graphon
−78	24.3	24.3
−89.5	23.7	24.9
−100	23.4	24.5
−111	22.7	24.1

At surface coverages $\theta > 1$, the adsorption data were plotted using the BET equation. Values of the Xe vapor pressure determined by Michels and Wassenaar (37) were used. Linear BET plots were obtained at all temperatures for both carbon blacks over the relative pressure range 0.05–0.20. The area σ occupied by a Xe atom in a complete monolayer was calculated using the nitrogen BET surface areas of 7.7 and 89.7 m.²/g. Table IV summarizes the results. On Sterling MT 3100 σ decreases with decreasing adsorption temperature. Values of σ on Graphon show no significant change with temperature. The average of the eight values in Table IV is 24.0 A,² which is in relatively good agreement with values reported in the literature for Xe adsorption on other surfaces (23, 38).

ACKNOWLEDGMENTS

The authors wish to thank Dr. W. A. Steele for very useful discussions, the A.E.C. for sponsoring the research under Contract No. AT(30-1)-1710, and the staff of the Pennsylvania State University Reactor Facility for irradiation of the uranyl nitrate hexahydrate.

REFERENCES

1. BEEBE, R. A., BISCOE, J., SMITH, W. R., AND WENDELL, C. B., *J. Am. Chem. Soc.* **69**, 95 (1947).
2. POLLEY, M. H., SHAEFFER, W. D., AND SMITH, W. R., *J. Phys. Chem.* **57**, 469 (1953).
3. SMITH, W. R., AND POLLEY, M. H., *J. Phys. Chem.* **60**, 689 (1956).

4. Griffiths, D. W. L., Thomas, W. J., and Walker, P. L., Jr. *Carbon* **1**, 515 (1964).
5. Ubbelohde, A. R., and Lewis, F. A., "Graphite and Its Crystal Compounds." Oxford University Press, 1960.
6. Roscoe, C., and Thomas, J. M., *Carbon* **4**, 383 (1966).
7. Graham, D., *J. Phys. Chem.* **61**, 1310 (1957).
8. Lopez-Gonzalez, J. de D., Carpenter, F. G., and Dietz, V. R., *J. Phys. Chem.* **65**, 1112 (1961).
9. Hobson, J. P., and Armstrong, R. A., *J. Phys. Chem.* **67**, 2000 (1963).
10. Clarke, J. T., *J. Phys. Chem.* **68**, 884 (1964).
11. Chènebault, P., and Schürenkämper, A., *J. Phys. Chem.* **69**, 2300 (1965).
12. Emmett, P. H., ASTM Techn. Publ. 51, pp. 95–105 (1941).
13. Friedman, H. C., M. S. Thesis, The Pennsylvania State University, State College, Pennsylvania, 1965.
14. Katcoff, S., and Rubinson, W., *Phys. Rev.* **91**, 1458 (1953).
15 Katcoff, S., *Nucleonics* **18**, 201 (1960).
16 Weinstein, A., and Friedman, H. C., *Rev. Sci. Instr.* **35**, 1083 (1964).
17 Alpert, D., *Rev. Sci. Instr.* **24**, 1004 (1953).
18 Liang, S. C., *J. Phys. Chem.* **57**, 910 (1953).
19 Pierce, C., *J. Phys. Chem.* **57**, 149 (1953).
20. Culver, R. V., and Watts, H., *Rev. Pure Appl. Chem.* **10**, 95 (1960).
21. Holmes, J. M., and Beebe, R. A., *J. Phys. Chem.* **61**, 1684 (1957).
22. Kobe, K. A., and Lynn, R. E., Jr., *Chem. Rev.* **52**, 117 (1953).
23. Cannon, W. A., *Nature* **197**, 1000 (1963).
24. Kuroda, H., and Akamatu, H., *Bull. Chem. Soc. Japan* **32**, 142 (1959).
25. Cannon, M. C., Grimes, W. R., Ward, W. T., and Watson, G. M., *Nucl. Sci. Eng.* **12**, 4 (1962).
26. Sams, J. R., Jr., Constabaris, G., and Halsey, G. D., Jr., *J. Phys. Chem.* **64**, 1689 (1960).
27. Peters, K., and Weil, K., *Z. Physik. Chem. (Leipzig)* **A148**, 1 (1930).
28. de Boer, J. H., and Kruyer, S., *Koninkl. Ned. Akad. Wetenschap. Proc.* **55B**, 451 (1952); *ibid.* **56B**, 67, 236, 415 (1953); *ibid.* **57B**, 92 (1954); *ibid.* **58B**, 61 (1955).
29. Ross, S., and Pultz, W. W., *J. Colloid Sci.* **13**, 397 (1958).
30. Kemball, S., *Advan. Catalysis* **2**, 233 (1950).
31. Young, D. M., and Crowell, A. D., "Physical Adsorption of Gases." Butterworths, London, 1962.
32. Hill, T. L., *Advan. Catalysis* **4**, 211 (1952).
33. Steele, W. A., *Advan. Colloid Interface Sci.* **1**, 3–78 (1967).
34. Hill, T. L., *J. Chem. Phys.* **14**, 441 (1946).
35. Cassel, H. M., *J. Phys. Chem.* **48**, 195 (1944).
36. Ross, S., and Clark, H., *J. Am. Chem. Soc.* **76**, 4291 (1954).
37. Michels, A., and Wassenaar, T., *Physica* **16**, 253 (1950).
38. Pritchard, J., *Nature* 194, 38 (1962).